v. 3, n. 61, 2023

International Journal of Health Science

IMAGING CRITERIA IN THE DIAGNOSIS OF ATELECTASIS

Hugo Patricio Peña Ochoa
Universidad Técnica de Machala
General practitioner
Ecuador
https://orcid.org/0000-0002-5438-6039

Luis Alonso Arciniega Jácome
Universidad Central del Ecuador
Doctor of Medical Sciences, PhD
Specialist in radiodiagnosis and imaging
Doctor of medicine and surgery
Ecuador
https://orcid.org/0000-0003-3617-5761

Sayda Valeria Ruilova Núñez
Universidad Técnica de Machala
General practitioner
Ecuador
https://orcid.org/0009-0002-6986-5339

Darwin Daniel Campos González
Universidad Técnica de Machala
General practitioner
Ecuador
https://orcid.org/0000-0002-4539-992X

María Belén Alvarado Mora
Universidad Técnica de Machala
General practitioner
Ecuador
https://orcid.org/0000-0001-6426-9058

Luis Edison Romero Gutierrez
Universidad Estatal de Guayaquil
General practitioner
Ecuador
https://orcid.org/0009-0008-7656-5952

Lissette Katherine Masache Gálvez
Universidad Técnica de Machala
General practitioner
Ecuador
https://orcid.org/0009-0009-6751-0295

Xiomara Jacqueline Fernández Lima
Universidad Técnica de Machala
General practitioner
Ecuador
https://orcid.org/0009-0007-2050-5515

Andrés Dennys Castillo Pedreros
Universidad Técnica de Machala
General practitioner
Ecuador
https://orcid.org/0009-0003-8964-5576

Carlos Aron Aguirre Cuasquer
Universidad Técnica de Machala
General practitioner
Ecuador
https://orcid.org/0009-0001-2481-7846

Karen Selena Sánchez Valladolid
Universidad Técnica de Machala
General practitioner
Ecuador
https://orcid.org/0000-0002-0969-9757

Dennys Fernando Méndez Rivera
Universidad Técnica de Machala
General practitioner
Ecuador
https://orcid.org/0009-0000-0536-125X

Abstract: Introduction: Atelectasis, defined as the collapse of the lung volume which is affected in its entirety or only a part of it, its classification is given by the etiology causing obstructive and non-obstructive atelectasis. The diagnosis of atelectasis includes observation and physical examination, which must be confirmed through imaging tests. Currently, the use of the different learning modalities reflects as a result a computer with the necessary data for the early recognition of atelectasis. **Objective:** Identify the imaging criteria present in atelectasis through a bibliographic review in the state of the art. **Methodology:** Narrative bibliographic review; analysis and interpretation of articles from various medical journals with a high impact on health. **Conclusion:** Signs of atelectasis present on plain chest radiography are direct and indirect signs; The increase in lung density and the deviation of the interlobar fissures with similar characteristics in the lower lobes but different in the upper lobes were reiterated. These 2 are considered direct signs. There are secondary signs to the loss of lung volume as compensation (indirect signs) among which the displacement of structures such as the trachea towards the affected side was observed when there is atelectasis of the upper lobe, the approximation of the ribs or elevation of the hemidiaphragm in cases of atelectasis in lower lobes. Another sign is the displacement of the hilum towards the upper part or the hyperinflation of a healthy segment or lobe that compensates for the compromise of the affected lung area. Artificial intelligence allows you to improve image quality, suppress structures and focus on a specific area through automatic segmentation.

Keywords: Lung collapse, lung collapse classification, radionuclide contrasted tomography, computed tomography, deep learning.

INTRODUCTION

One of the entities of alveolar affection is atelectasis, which derives from the Greek "ateles" which means incomplete and "ektasis" expansion or stretching, defined as the decrease in volume that affects the lung in its entirety or only a part of it, that is, a collapse either of a specific, total or partial area of the lung (Domino, 2019).

In the epidemiological field, there is no record of incidence or prevalence of atelectasis worldwide, however, there are records of diseases that cause atelectasis, related to their etiology, which classifies them as obstructive and non-obstructive (Pritchett et al., 2021).

Intra or postoperative atelectasis generally causes mucus to accumulate and obstruct the bronchial lumen, representing between 1 and 20% of patients in prolonged surgeries (Thorpe et al., 2020). In a study carried out in Ecuador, there are data on nosological entities that cause atelectasis, finding atelectasis in neonates with less than 1500 g of adhesive cause, which is one of the non-obstructive atelectasis, with an incidence of 60%, while, in the adult population there is a predominance of obstructive atelectasis (Malloy & Mcgovern, 2018).

Within the bibliography there are various classifications of atelectasis, the most common being atelectasis due to obstruction, compression, and atelectasis due to scarring or contraction (restrictive) (Santos. A, 2019); The obstructive is the most common, given as a result of an obstruction in the airway between the trachea and the alveoli, it can be given by a mucus plug, a tumor that compresses or obstructs the light of the airway or by a foreign body. It is considered one of the most frequent postoperative respiratory complications (Bradley et al., 2021).

Compression atelectasis is caused by loss of contact of the pleurae, as occurs in the case of passive atelectasis, resulting in loss of contact of the pleurae when there is a pleural effusion or pneumothorax (Sum et al., 2019).). Pulmonary fibrosis causes contraction atelectasis, another condition is caused by the loss or inactivation of surfactant that is common in the pediatric population due to prematurity, lung immaturation, or the inability to secrete pulmonary surfactant by type II pneumocytes (McPherson & Wambach, 2018).

The symptoms depend on the progression of the bronchial obstruction. If it is slow, it is usually present with minor symptoms, as in the middle lobe syndrome, which is usually asymptomatic. However, when the affectation includes the right middle and lower lobe, it usually presents with an unexplained cough. productive, dry but severe (Valdés Bécares et al., 2018). If the progression of the obstruction is established quickly, an immediate collapse of the lung occurs, causing dyspnea that is accompanied by cyanosis, in addition to pain on the affected side of moderate intensity (Sun et al., 2021).

The diagnosis of atelectasis includes the formulation of a hypothesis through observation and physical examination, which has to be corroborated through complementary examinations, mainly imaging (Yin et al., 2021).

D - learning or Digital learning represents any type of learning facilitated by the use of technology, it includes electronic learning (E learning) and mobile learning (M learning), the first for being learning that is supported by digital tools through electronics, the second is a subset of E-learning and is defined by the use of technology such as mobile devices to facilitate and/or improve learning (Kumar Basak et al., 2018).

These learning methods have been carried out thanks to artificial intelligence (AI) and the improvement of the devices themselves, which have the capacity to learn and improve

their analysis through the use of computational algorithms (Machine Learning) (Helm et al., 2020), through its subset called Deep Learning or deep learning, which is reflected in the introduction of various processing layers or algorithms to an electronic medium or computer (Bharati et al., 2020).

Currently, the use of different learning modalities is increasing in the world and several studies reflect as a result a computer with the necessary data for early recognition and with greater precision to stratify, plan imperceptible differential diagnoses for medical personnel in a first analysis(Chassagnon et al., 2020); or suggest a prognosis of various pathologies that affect the respiratory tract and cause lung collapse at the lobar level or in some segment (Erickson et al., 2017).

Under this contextual framework, the present work aims to identify the imaging criteria present in atelectasis through a bibliographic review in the last 5 years in the Pubmed database and other high-impact medical journals, which allows medical personnel to achieve recognition of this condition in an effective way through this update.

DEVELOPMENT

The use of complementary tests linked to imaging is fundamentally based on knowledge of radiological anatomy, which provides data for the correct description of lesions (Wilson et al., 2018).

RADIOLOGICAL ANATOMY

There are different radiological densities that represent water, metallic density, calcium, fat and gas, which are distributed in the body (Warren et al., 2018).

TRACHEOBRONCHIAL TREE

The trachea is represented by an extension from the larynx to the main bronchi, its shape is a cylindrical tube; its cervical portion is in the midline, however, the portion of the trachea in the intrathoracic region deviates slightly to the right side and as it descends it goes backwards (Unger & Bogaert, 2017). The aortic arch compresses the left wall in its lateral portion, in older adults it is a radiological sign that is marked by progression of aortic elongation and its diagnostic differentiation is important because it also usually causes dyspnea (Regmi et al., 2021).

The ramification of the bronchial system is asymmetric, the left main bronchus is longer and less vertical than the right, on the left side there are 2 lobar bronchi, while on the right side there are three; Regarding the segmental bronchi, there are eight bronchi on the left side and ten on the right side (Petite Felipe et al., 2021).

LOBAR AND SEGMENTAL PULMONARY ANATOMY

The major fissure divides the left lung into 2 lobes, superior and inferior, the upper lobe is subdivided into 5 segments (upper and inferior lingular segment, anterior, apicoposterior I and apicoposterior II), the bronchus is divided into 2 branches, 1 superior and another lingular (Gordienko et al., 2019). The lower lobe is divided into 4 segments (superior and anterior basal, posterior basal, and lateral basal), differentiating their segmentation enables medical personnel to identify the affected area of the lung (Mittal et al., 2017).

The right lung is fragmented by the major and minor fissure, observing 3 lobes, in the lower lobe there are 4 segments comprised of 3 basal segments (posterior, lateral, and anterior basal) and 1 upper segment (Marini, 2019). The middle lobe is comprised of 2

segments (lateral and medial segments), finally, the apical, posterior and anterior segments constitute the upper lobe, frequently affected post Covid - 19, demonstrated in a spirometric and radiological study in 65 patients (Bardakci et al. al., 2021).

SUBSEGMENTAL PULMONARY ANATOMY

Identifiable in computed tomography (CT), made up of acini and the secondary pulmonary lobule, within them is the bronchiole and arteriole, these lobules are separated by septa that present lymphatic vessels and veins as content (Ruaro et al., 2021).

ATELECTASIS

Affection of the lung tissue in any portion characterized by tissue collapse or incomplete expansion, which is caused by resistance to the entry of air into the alveoli (Grott et al., 2022).

TYPES OF ATELECTASIS

Various entities can cause atelectasis, whether pulmonary or extrapulmonary, in addition to predisposing factors such as occurs in patients with morbid obesity undergoing abdominal surgery where 7.6% presented atelectasis in a study carried out in 2020, there are various ways to classify the type of atelectasis according to its cause(Chandler et al., 2020).

DIAGNOSIS

PLAIN X-RAY OF THE THORAX

X-ray equipment is used, which, through the use of radiation by means of energy waves, results in images of the body in its internal part due to the absorption of radiation in different amounts, showing an x-ray with colors in white., black and gray (Foley et al., 2021).

In thoracic disease entities, initial imaging studies are simple, mostly using lateral and posteroanterior (PA) radiographs; however, there are variations that can offer help depending on the part of the chest affected (Gu et al., 2021).

Oblique X-rays: It is used when focal opacities have been visualized in the postero-anterior modality. Its advantage lies in avoiding the superimposition of the anatomical structures observed in the postero-anterior radiography and to rule out images similar to a pulmonary nodule that can be perceived in an image. lateral(Kundu et al., 2021).

Exhalation X-rays: Air entrapment and pneumothorax that encompasses a minimal part of the lung are generally detected, although chest X-ray in inspiration is the technique of choice for chest X-ray, since there are no better benefits in exhalation (Cases Susarte et al., 2017).

Portable or dorsal decubitus radiography: Useful when mobilization of the patient is contraindicated in blunt trauma, it is performed in a PA shot, although various studies show that emergency ultrasound (FAST or Focused Assessment with Sonography in Trauma) has a sensitivity of 67% in parallel with chest X-ray 54% (Stengel et al., 2020).

X-ray with horizontal beam in lateral decubitus (PANCOAST): It allows the identification of fluid in the pleural cavity in quantities of 50 ml and/or greater, however, studies corroborate that in the ultrasound pleural effusion is detectable from 20 ml (Ibitoye et al. al., 2018).

The various modalities for taking X-rays must meet criteria for correct taking, among which the following stand out:

The location of the shoulder blades, which must project outside the lung fields, the patient must be located in front, where the clavicles in their portion of the internal ends are at the same distance from the spinous processes (Baratella et al., 2021).

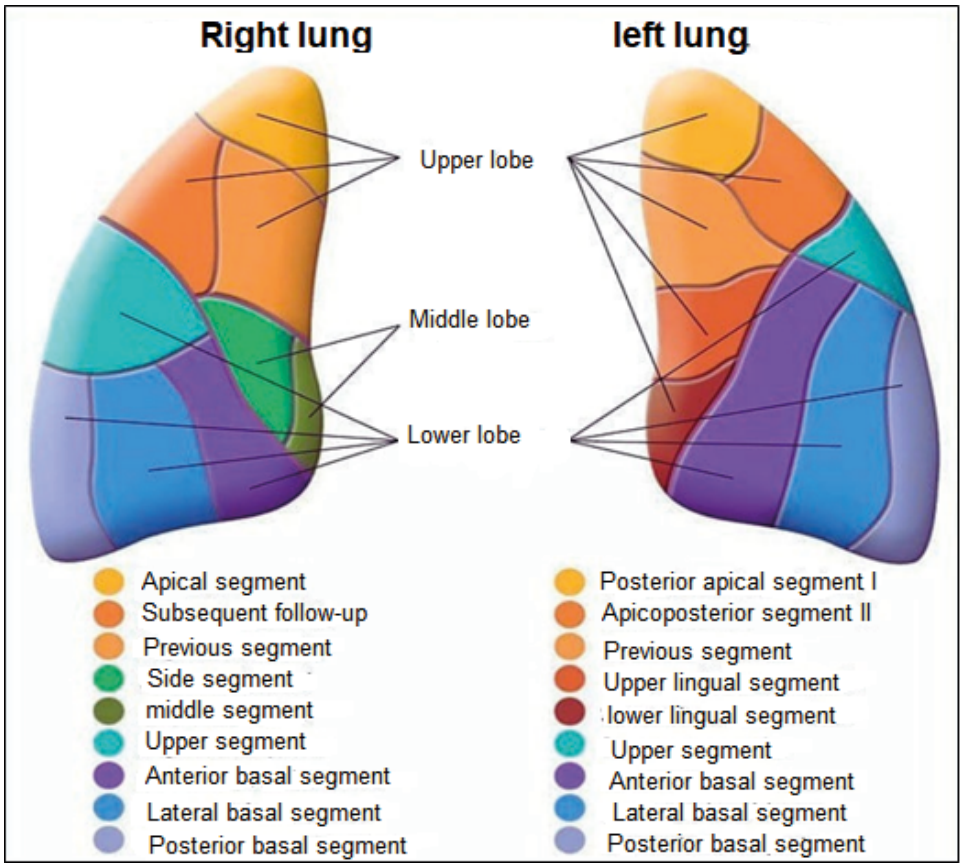

Figure 1. *Segmental lung anatomy.*

Taken from: Schuenke, Michael; Schulte, Erik; Schumacher U. Thieme Atlas of Anatomy - Internal organs [Homepage on the Internet]. 3rd ed. India: Thieme Publishers Delhi, 2020; Available from: https://www.thieme.com/books-main/anatomy/product/5566-internal-organs-thieme-atlas-of-anatomy

ATELECTASIS DUE TO OBSTRUCTION OR REABSORPTION	
EXTRINSIC	**INTRINSIC**
CONGENITAL MALFORMATIONS	TUBERCULOSIS
MEDIASTINAL TUMORS	PNEUMONIA
LADENOPATHIES	MUCUS PLUGS
VASCULAR MALFORMATIONS	- CYSTIC FIBROSIS
- ANEURYSMS	- LUNG ABSCESS
	- ASTHMA
	- BRONCHIECTASIS.
	- POSTOPERATIVE IN PROLONGED SURGERY

CONTRACTION ATELECTASIS	
BRONCHOPULMONARY DYSPLASIA	NEUROMUSCULAR DISORDERS
TUBERCULOSIS	PULMONARY FIBROSIS
COMPRESSION ATELECTASIS	
CONGENITAL MALFORMATIONS	PLEURAL EFFUSION
LADENOPATHIES	INTRATHORACIC TUMORS
PNEUMOTHORAX	TENSION PNEUMATOCELE.
ADHESIVE ATELECTASIS	
DEFICIENCY OR INACTIVATION OF PULMONARY SURFACTANT.	

Table 1. Types of atelectasis by its cause.

Taken from: Lou Q, Zhang S-X, Yuan L. Clinical analysis of adenovirus pneumonia with pulmonary consolidation and atelectasis in children. J Int Med Res [homepage on the Internet] 2021;49(2):300060521990244.

Available from: http://www.ncbi.nlm.nih.gov/pubmed/33530809

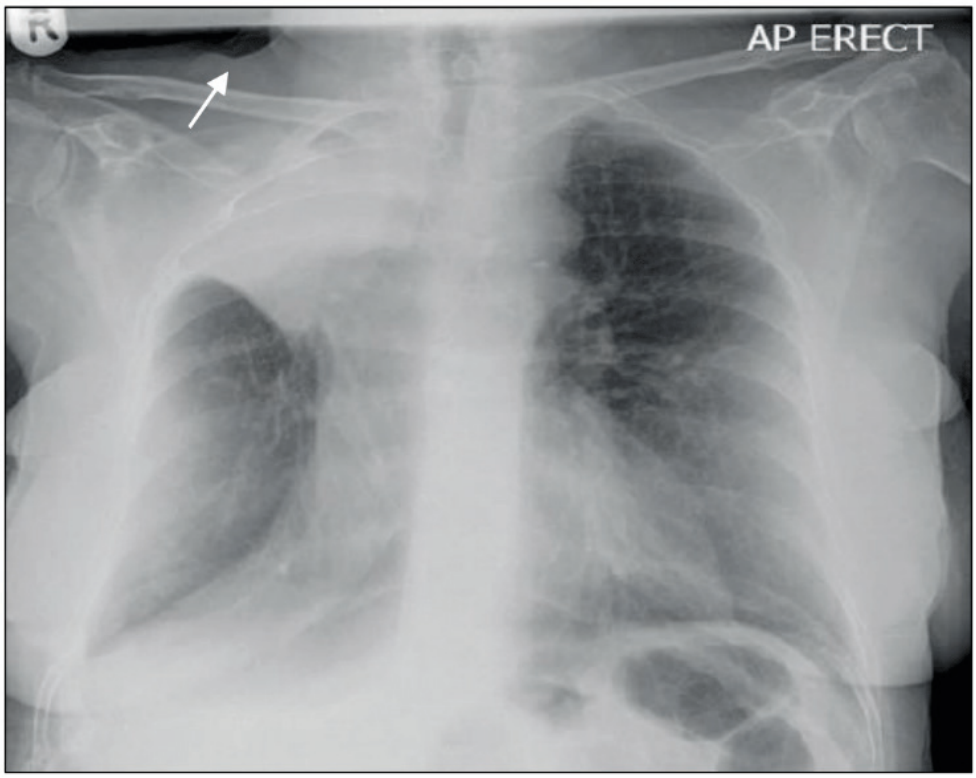

Figure 2. *Collapsed right upper lobe. Increased density at the level of the right lung apex, displacement of the major fissure (Arrow: "Golden's S" sign), displacement of the trachea towards the affected side.*

Taken from: Bansal T, Beese R. Interpreting a chest X-ray. Br J Hosp Med [homepage on the Internet] 2019;80(5):C75–C79.

Available from: http://www.magonlinelibrary.com/doi/10.12968/hmed.2019.80.5.C75

Prior to taking, the examination must be carried out in a maximum and sustained inspiration which allows visualization above the diaphragmatic domes of the sixth costal arch in its anterior portion (Shekhda, 2020). Visualize dorsal column posterior to the mediastinum and retrocardiac vessels under a high kilovoltage which allows correct penetration of the radiograph (Pogue & Wilson, 2018).

In the posteroanterior (PA) shot, it smust allow visualization of the lateral costophrenic sinuses and the pulmonary apices, while in the lateral view the sternum and the costophrenic sinuses in its posterior portion must be observed (Bansal & Beese, 2019).

Radiology has been used digitally through techniques in computed tomography, magnetic resonance, ultrasound and scintigraphy, which have enabled a greater transmission capacity towards a monitor, where the required image can provide greater contrast resolution (Ugalde et al. al., 2021).

RADIOLOGICAL PATTERNS IN ATELECTASIS

There is a variety depending on the involvement of the lobe in the lung, the atelectasis that takes the lower lobe of the lung is generally similar, while the atelectasis that occurs in the upper lobe are different (Lin et al., 2021).

Left lower lobe (LII) and right lower lobe (LID): In the usual modalities it is observed: on the side, a triangle-shaped density pointing the hilum with the vertex. In addition, in the posteroanterior opacification is observed at the paravertebral level which erases the diaphragm, the major fissure is slightly displaced posteriorly and makes the lower part (Maki et al., 2020).

Middle lobe: Atelectasis at this level causes the major fissure to shift upwards, while the minor fissure is deviated inferiorly (Protić et al., 2020).

Left upper lobe (LSI): Diagnosis is complicated in the posteroanterior view, there is blurring of the edge of the heart due to increased density. The difference lies in the absence of the minor fissure, there is an anterior displacement of the major fissure and the collapse of the lobe forwards (Assallum et al., 2019).

Right upper lobe (RSL): On the lateral radiograph, half of the major fissure is displaced anteriorly and the minor fissure is elevated. In PA, there is an opacification at the level of the paramediastinum, caused by internal displacement and towards the upper part of the atelectatic lobe, generating the sign called "Golden's S" (Lou et al., 2021).

In a study of 58 patients showing perihilar atelectasis on a chest X-ray, 21 of them were shown to have an obstructing tumor as the primary cause (Ozturk et al., 2018). In addition, thick perihilar linear atelectasis best seen on a computed tomography (CT) scan, suggests a diagnosis of primary lung cancer (Chung et al., 2018).

Within artificial intelligence, the massively trained artificial neural network (MTANN) (Takimoto et al., 2020), and the convolutional neural network (CNN) allow the collection of data which improves the image in a chest X-ray by giving options such as separating bone components for better visualization of the lung fields (Suzuki, 2017).

POSITRON EMISSION TOMOGRAPHY AND COMPUTERIZED TOMOGRAPHY (PET/CT)

One of the most modern diagnostic methods, is part of nuclear medicine, used simultaneously gives a great advantage for the detection, stratification of neoplasms (Hedenstierna et al., 2020); and the evaluation of response in patients with some type of lung

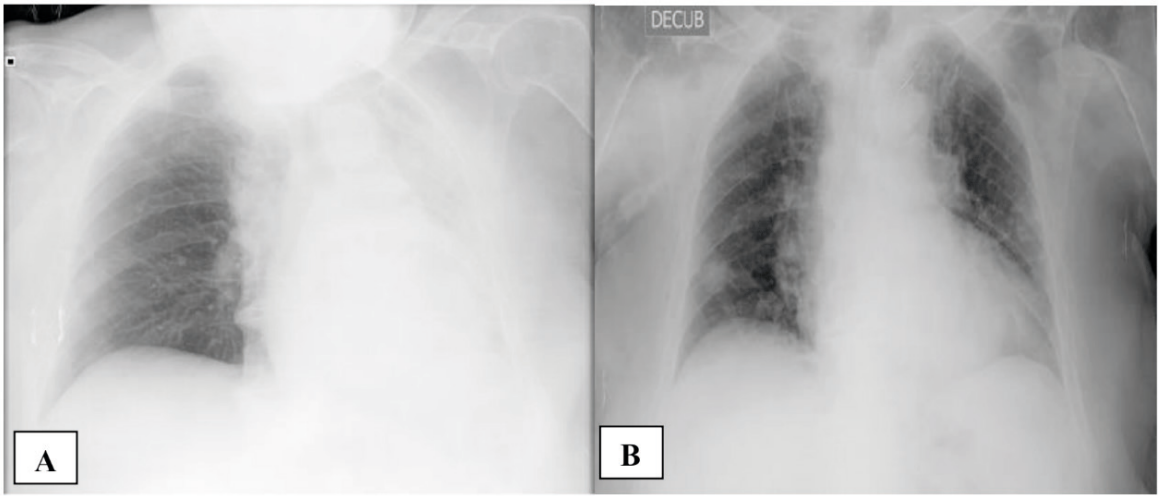

Figure 3. *Older adult with increased density in the left hemithorax and deviation of the mediastinum towards the affected side (A). Image (B), older adult 48 hours after treatment with mucolytics and bronchodilators.*

Taken from: Valdés Bécares J, Martínez García P, Maderuelo Riesco I. Atelectasis due to mucus plug resolved conservatively. Primary Care [homepage on the Internet] 2018;50(9):562–563.

Available from: https://doi.org/10.1016/j.aprim.2018.03.006

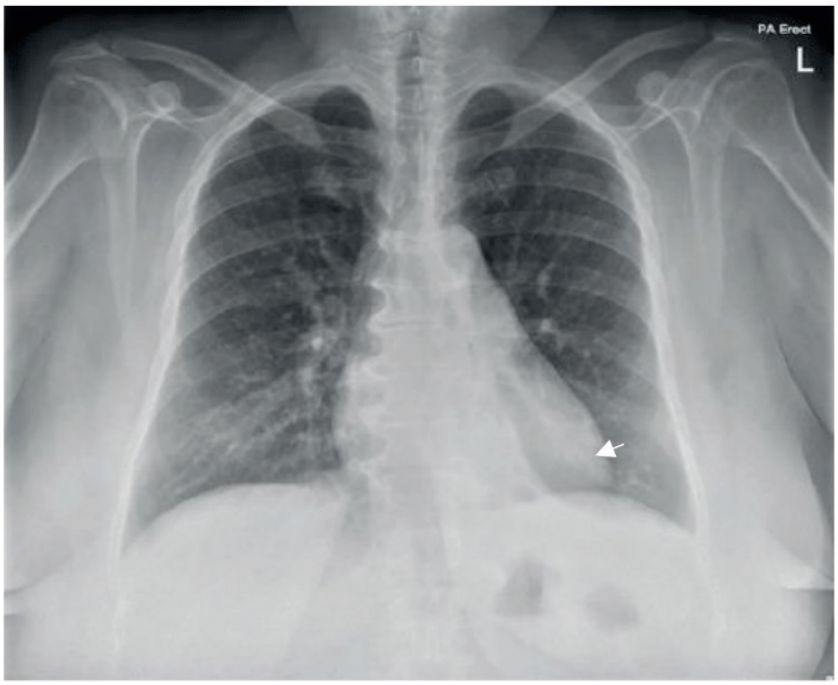

Figure 4. *Collapsed lower left lobe. A triangle with its apex towards the hilum can be seen faintly through the cardiac silhouette (Arrow).*

Taken from: Bansal T, Beese R. Interpreting a chest X-ray. Br J Hosp Med [homepage on the Internet] 2019;80(5):C75–C79.

Available from: http://www.magonlinelibrary.com/doi/10.12968/hmed.2019.80.5.C75

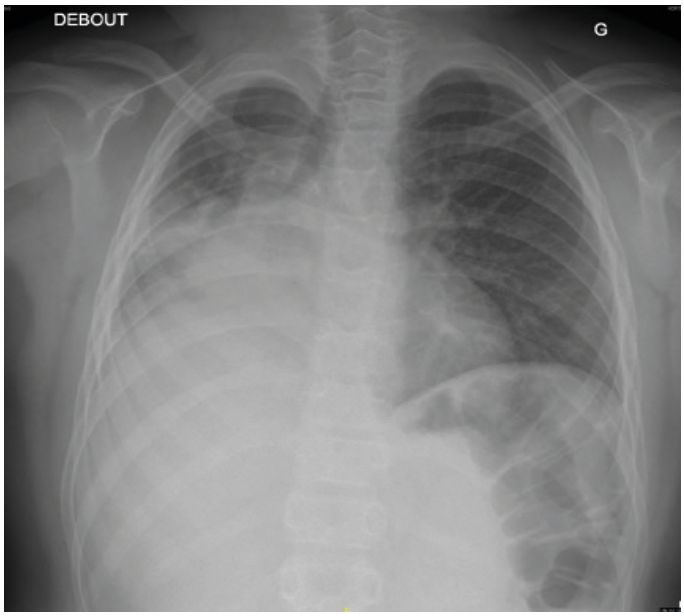

Figure 5. *Chest x-ray of an 8-year-old schoolboy after a traffic accident, an increase in density is observed at the level of the lower and middle lobe of the right lung (atelectasis), tracheal deviation, displacement of fissures towards the upper part due to presumed pulmonary contusion.*

Taken from: Berland M, Oger M, Cauchois E, Retornaz K, Arnoux V, Dubus J. Pulmonary contusion after bumper car collision: Case report and review of the literature. Respir Med Case Reports [homepage on the Internet] 2018;25(October):293–295.

Available from: https://doi.org/10.1016/j.rmcr.2018.10.006

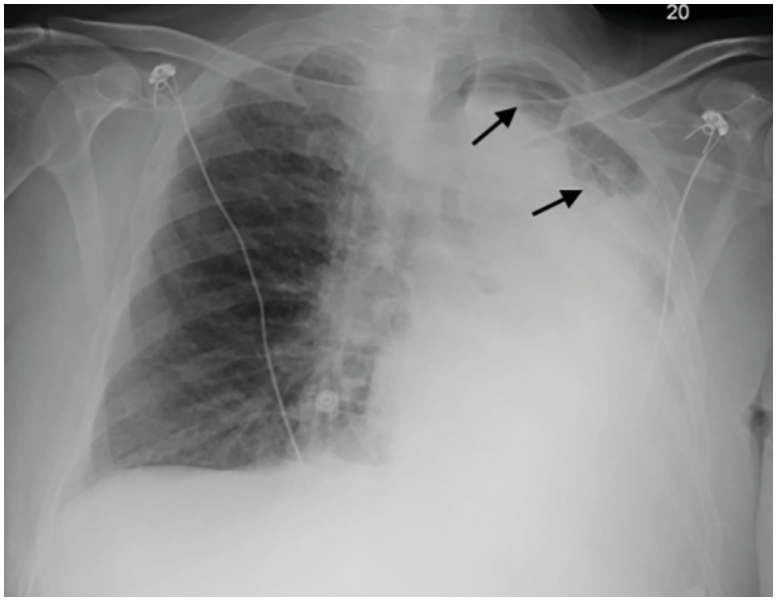

Figure 6. *Post-bronchoscopy chest X-ray (4 sessions), an increase in lung density is observed in the left hemithorax, hyperinflation of the apicoposterior segment as compensation.*

Taken from: Assallum H, Song TY, DeLorenzo L, Harris K. Bronchoscopic instillation of DNase to manage refractory lobar atelectasis in a lung cancer patient. Ann Transl Med [homepage on the Internet] 2019;7(15):363.

Available from: http://www.ncbi.nlm.nih.gov/pubmed/31516909

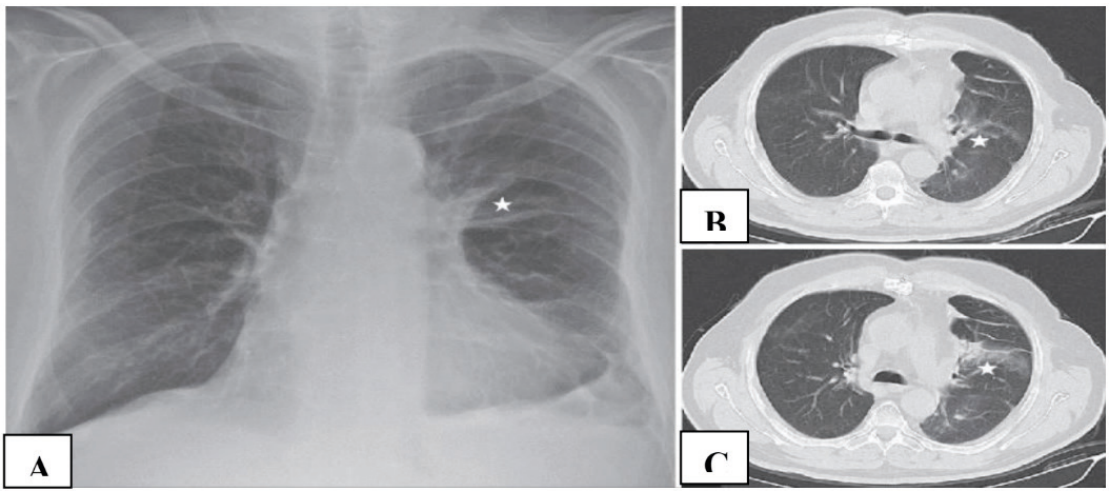

Figure 7. *Chest X-ray showing left perihilar collapse displacing the hilum slightly superiorly (A). Chest computed tomography (B and C) confirms linear atelectasis (asterisk) due to obstructive bronchogenic carcinoma.*

Taken from: Ozturk K, Soylu E, Topal U. Linear Atelectasis around the Hilum on Chest Radiography: A Novel Sign of Early Lung Cancer. J Clin Imaging Sci [homepage on the Internet] 2018;8(1):27.

Available from: http://www.ncbi.nlm.nih.gov/pubmed/30123672

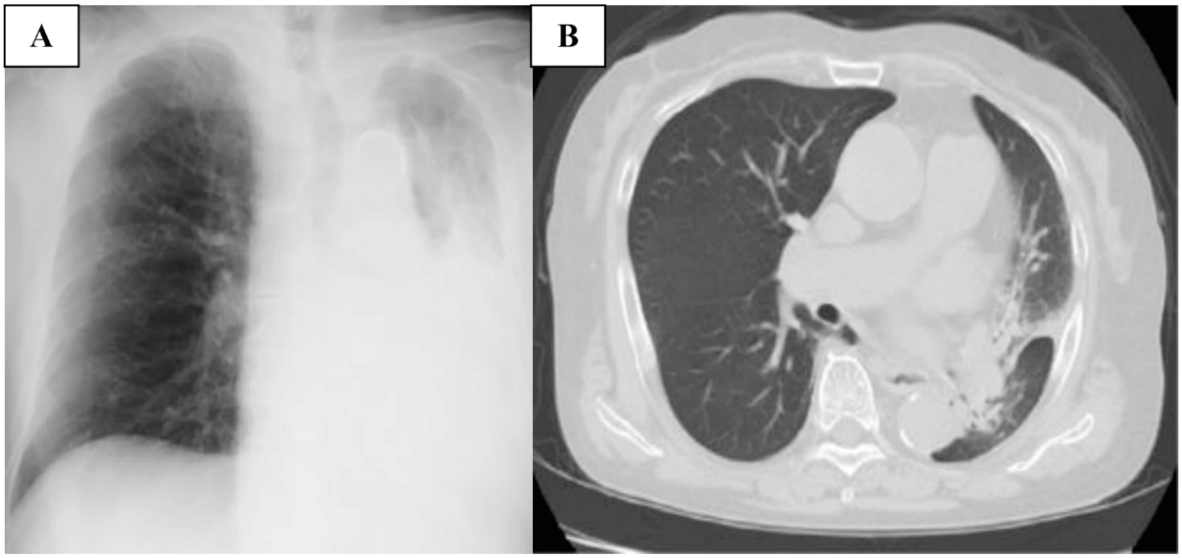

Figure 8. *A la izquierda **(A)** hemitórax izquierdo con aumento de la densidad pulmonar y desviación traqueal hacia hemitórax afecto. Tomografía computarizada **(B)** colapso de pulmón izquierdo por impactación de moco en bronquio principal izquierdo.*

Taken from: Takimoto T, Kagawa T, Tachibana K, Arai T, Inoue Y. Massive atelectasis by mucoid impaction in an asthma patient during treatment with anti-interleukin-5 receptor antibody. Respirol case reports [homepage on the Internet] 2020;8(6):e00599.

Available from: http://www.ncbi.nlm.nih.gov/pubmed/32566229

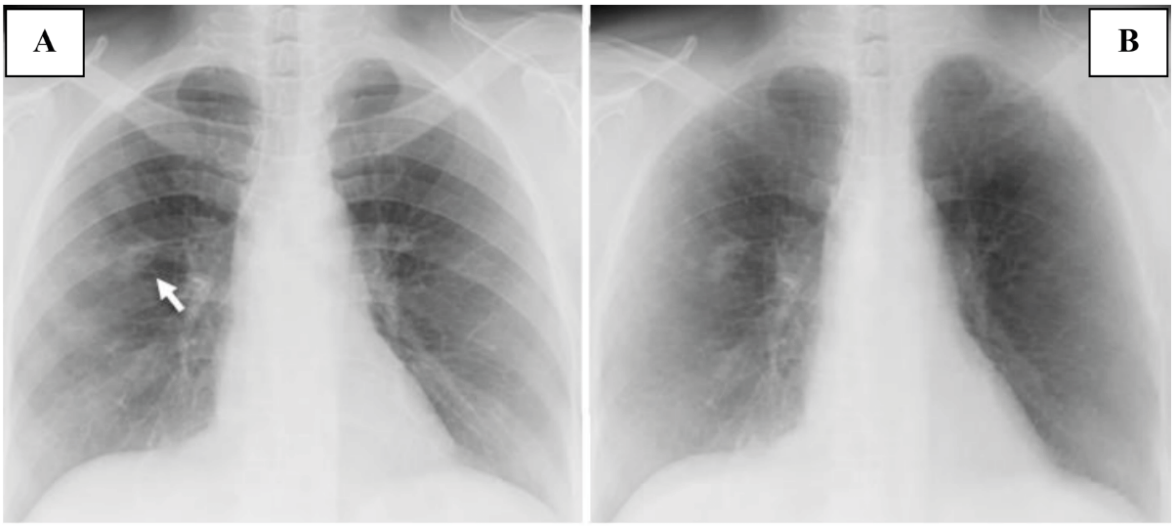

Figure 9. *Separation of soft tissue and bone tissue by using artificial intelligence. (A) A nodule is observed at the level of the right pulmonary hilum (arrow). (B) After the processing and use of neural networks, the bone tissue is decreased for better visualization of the nodule.*

Taken from: Suzuki K. Overview of deep learning in medical imaging. Radiol Phys Technol [homepage on the Internet] 2017;10(3):257–273.

Available from: https://pubmed.ncbi.nlm.nih.gov/28689314/

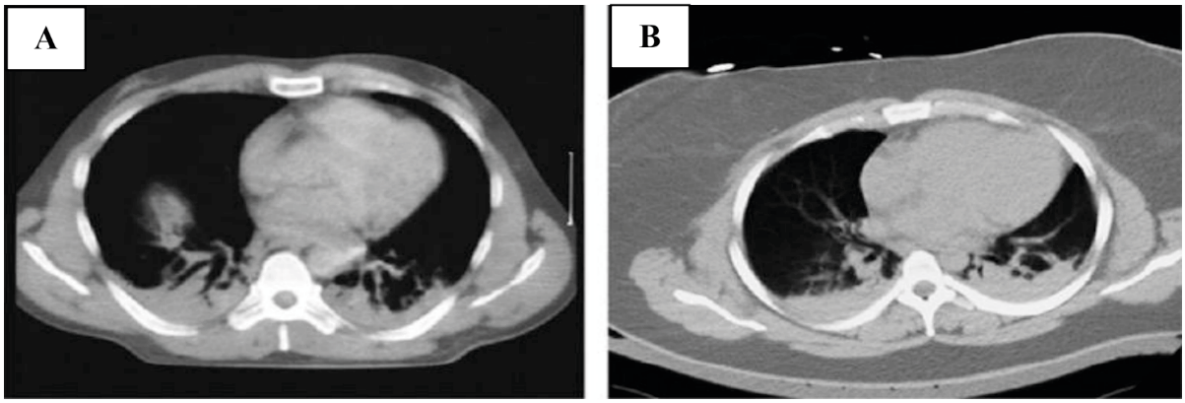

Figure 10. *(A) Hyperdense image in the lung area that represents atelectasis, there is a hyperdense area near the center of the right lung which represents the diaphragmatic dome in its upper area (diaphragmatic elevation).* ***(B)*** *Patient with BMI 43 kg/m2, with hyperdense image within the lung fields representing lung collapse (Hedenstierna et al., 2020).*

Taken from: Hedenstierna G, Tokics L, Reinius H, Rothen HU, Östberg E, Öhrvik J. Higher age and obesity limit atelectasis formation during anaesthesia: an analysis of computed tomography data in 243 subjects. Br J Anaesth [homepage on the Internet] 2020;124(3):336–344.

Available from: https://linkinghub.elsevier.com/retrieve/pii/S0007091219309304

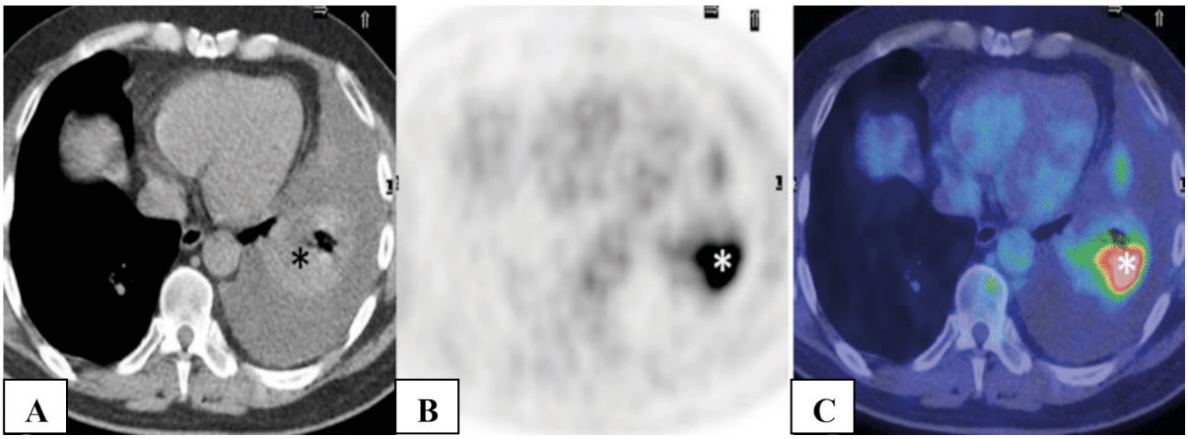

Figure 11. *A 64-year-old male, exposed to asbestos (A) CT mediastinal window, a collapse of the lower lobe (asterisk) is observed in the left hemithorax accompanied by pleural effusion. (B) Axial PET shows intense focal metabolic activity (asterisk) in the lower lobe of the left lung. (C) Fused axial PET/CT shows 18F-FDG uptake due to the presence (asterisk) of a pulmonary nodule within an atelectasis of the left lower lobe, suggestive of malignancy.*

Taken from: Gorospe L, Jover-Díaz R, Muñoz-Molina GM, Cabañero-Sánchez A, Gambí-Pisonero E, Barbolla-Díaz I. Round atelectasis: PET/CT findings. Intern Emerg Med [homepage on the Internet] 2018;13(7):1127–1128.

Available from: https://doi.org/10.1007/s11739-018-1867-1

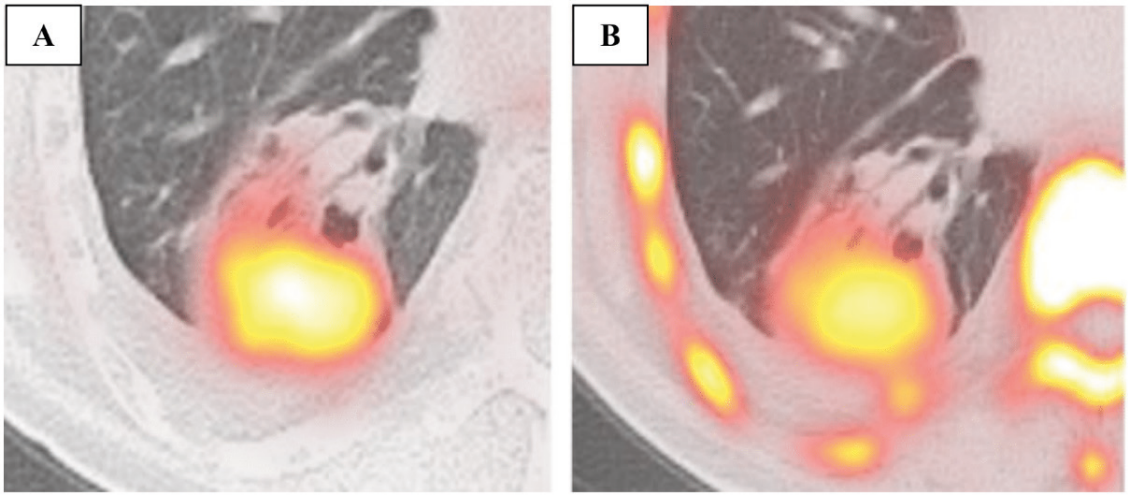

Figure 12. (A) *The use of 18F – FDG showed uptake (hypermetabolic activity) by the mass in the right lung, it did not uptake atelectatic areas around the presumed nodule. (B) Image using 18 F – FLT shows greater uptake by the mass, but also presents hypermetabolic activity in benign lesions.*

Taken from: Norikane T, Yamamoto Y, Mitamura K, Tani R, Nishiyama Y. False-Positive 18F-FDG and 18F-Fluorothymidine Uptake in a Patient With Round Atelectasis. Clin Nucl Med [homepage on the Internet] 2020;45(3):e158–e159.

Available from: http://www.ncbi.nlm.nih.gov/pubmed/31833928

cancer or at the level of other organs (Fonti et al., 2019). In a study carried out in Bogotá, asymptomatic oncological patients with Covid 19 were found with the use of PET/CT (Martí et al., 2020).

18 F – fluorodeoxyglucose (18F – FDG) is a radiopharmaceutical, classified as a glucose analogue which is used for this imaging study due to its ability to bind to tumor cells (Brodin et al., 2020). Studies of 18 F – fluorodeoxyglucose (18F – FDG) have intensified in the last five years, reaching dose results for its use that allow local control of the tumor (Bai et al., 2021). In a prospective clinical trial it was concluded that 18F - FLT (18F-fluorothymidine) is less specific than 18F - FDG for the diagnosis of patients with atelectasis due to lung cancer undergoing radiotherapy (Christensen et al., 2021).

Lung cancer (CA) has been divided into 2: small cell CA and non-small cell CA with an incidence of 15% and 85% respectively in Europe and the United States (Bade & Dela Cruz, 2020). In a study of 67 patients who were undergoing their fifth week of radiotherapy, they underwent a PET/CT scanner, in which it was possible to verify its accuracy and reliability in delimiting tumors and excluding anomalies that are not of a tumor nature, such as atelectasis (Ganem et al. al., 2018).

The Hounsfield units used in computed tomography are highly relevant for the detection of atelectasis, a normal lung ranges from (-850 ± 65 HU) (Mascalchi et al., 2017). Various studies confirm a lung atelectasis has higher Hounsfield units (-380 ± 185 HU) than a normal lung, but they also have a lower range in malignant tissue (35 ± 20 HU) (Tamura et al., 2021).

The use of 18F - FDG uptake has notable differences (Gorospe et al., 2018), according to a study in 21 patients (13 men and 8 women) who presented atelectasis on CT, the intensity of 18F - FDG uptake was lower in patients with malignancies, but remained higher than in a normal lung (Norikane et al., 2020).

CONCLUSIONS

There are various causes that cause atelectasis, whether obstructive or non-obstructive, it is important to associate the risk factors presented by the patient for a diagnostic suspicion of the underlying disease.

The physical examination is an important role for the diagnosis of pulmonary pathology, however, there are usually minimal affectations that go unnoticed by health personnel. Complementary examinations linked to imaging are indicated for the detection of lobar or segmental atelectasis, especially simple chest radiology, which is the most recommended.

Among the radiological signs present in the simple chest X-ray, the increase in lung density and the deviation of the interlobar fissures with similar characteristics in the lower lobes but different in the upper lobes were reiterated; these 2 are considered as direct signs.

There are signs that represent secondary data to the loss of lung volume as compensation (indirect signs) among which the displacement of structures such as the trachea towards the affected side was observed when there is atelectasis of the upper lobe, the approximation of the ribs or elevation of the hemidiaphragm in cases of atelectasis in the lower lobes. Another sign is the displacement of the hilum towards the upper part or the hyperinflation of a healthy segment or lobe that compensates for the compromise of the affected lung area.

The most advanced studies include computed tomography, magnetic resonance and positron emission tomography in which the cause of atelectasis is identified and allows an adequate therapeutic approach. In the CT a slight hyperdensity of the collapsed area of

the lung is noted, the Hounsfield units can measure and draw a difference between a normal lung, collapsed and with malignant tumor pathology.

AI plays an important role and is in constant evolution, the machines used for the imaging study of lung pathology allow to improve the quality of the image, suppress structures to focus the study on a specific area, verify the compromised area of the lung by means of automatic segmentation.

The studies given by positron emission tomography and computed tomography (PET/CT) have allowed the early detection of lung cancer worldwide and have improved the treatment approach allowing timely changes such as dose adjustment.

REFERENCES

Assallum, H., Song, T. Y., DeLorenzo, L., & Harris, K. (2019). **Bronchoscopic instillation of DNase to manage refractory lobar atelectasis in a lung cancer patient.** *Annals of Translational Medicine*, *7*(15), 363. https://doi.org/10.21037/atm.2019.05.15

Bade, B. C., & Dela Cruz, C. S. (2020). **Lung Cancer 2020: Epidemiology, Etiology, and Prevention**. *Clinics in Chest Medicine*, *41*(1), 1–24. https://doi.org/10.1016/j.ccm.2019.10.001

Bai, Y., Xu, J., Chen, L., Fu, C., Kang, Y., Zhang, W., Fakhri, G. E., Gu, J., Shao, F., & Wang, M. (2021). **Inflammatory response in lungs and extrapulmonary sites detected by [18F] fluorodeoxyglucose PET/CT in convalescing COVID-19 patients tested negative for coronavirus.** *European Journal of Nuclear Medicine and Molecular Imaging*, *48*(8), 2531–2542. https://doi.org/10.1007/s00259-020-05083-4

Bansal, T., & Beese, R. (2019). **Interpreting a chest X-ray.** *British Journal of Hospital Medicine*, *80*(5), C75–C79. https://doi.org/10.12968/hmed.2019.80.5.C75

Baratella, E., Marrocchio, C., Bozzato, A. M., Roman-Pognuz, E., & Cova, M. A. (2021). **Chest X-ray in intensive care unit patients: what there is to know about thoracic devices.** *Diagnostic and Interventional Radiology (Ankara, Turkey)*, *27*(5), 633–638. https://doi.org/10.5152/dir.2021.20497

Bardakci, M. I., Ozturk, E. N., Ozkarafakili, M. A., Ozkurt, H., Yanc, U., & Yildiz Sevgi, D. (2021). **Evaluation of long-term radiological findings, pulmonary functions, and health-related quality of life in survivors of severe COVID-19.** *Journal of Medical Virology*, *93*(9), 5574–5581. https://doi.org/10.1002/jmv.27101

Bharati, S., Podder, P., & Mondal, M. R. H. (2020). **Hybrid deep learning for detecting lung diseases from X-ray images.** *Informatics in Medicine Unlocked*, *20*(January), 100391. https://doi.org/10.1016/j.imu.2020.100391

Bradley, S. H., Bhartia, B. S., Callister, M. E., Hamilton, W. T., Hatton, N. L. F., Kennedy, M. P., Mounce, L. T., Shinkins, B., Wheatstone, P., & Neal, R. D. (2021). **Chest X-ray sensitivity and lung cancer outcomes: a retrospective observational study.** *The British Journal of General Practice : The Journal of the Royal College of General Practitioners*, *71*(712), e862–e868. https://doi.org/10.3399/BJGP.2020.1099

Brodin, N. P., Tomé, W. A., Abraham, T., & Ohri, N. (2020). **18F-Fluorodeoxyglucose PET in Locally Advanced Non-small Cell Lung Cancer: From Predicting Outcomes to Guiding Therapy.** *PET Clinics*, *15*(1), 55–63. https://doi.org/10.1016/j.cpet.2019.08.009

Cases Susarte, I., Sánchez González, A., & Plasencia Martínez, J. M. (2017). **Should we perform an inspiratory or an expiratory chest radiograph for the initial diagnosis of pneumothorax?** *Radiologia*, *60*(5), 437–440. https://doi.org/10.1016/j.rx.2017.10.004

Chandler, D., Pham, A. D., Resident, A., Okada, L. K., Student, M., Kaye, R. J., Student, M., Cornett, E. M., Fox, C. J., Urman, R. D., Kaye, A. D., & Academic, C. (2020). **Best Practice & Research Clinical Anaesthesiology Perioperative strategies for the reduction of postoperative pulmonary complications.** *Best Practice & Research Clinical Anaesthesiology*, *xxxx*, 1–14. https://doi.org/10.1016/j.bpa.2020.04.011

Chassagnon, G., Vakalopolou, M., Paragios, N., & Revel, M.-P. (2020). **Deep learning: definition and perspectives for thoracic imaging.** *European Radiology*, *30*(4), 2021–2030. https://doi.org/10.1007/s00330-019-06564-3

Christensen, T. N., Langer, S. W., Persson, G., Larsen, K. R., Loft, A., Amtoft, A. G., Berthelsen, A. K., Johannesen, H. H., Keller, S. H., Kjaer, A., & Fischer, B. M. (2021). **18F-FLT PET/CT Adds Value to 18F-FDG PET/CT for Diagnosing Relapse After Definitive Radiotherapy in Patients with Lung Cancer: Results of a Prospective Clinical Trial.** *Journal of Nuclear Medicine : Official Publication, Society of Nuclear Medicine*, *62*(5), 628–635. https://doi.org/10.2967/jnumed.120.247742

Chung, J. H., Richards, J. C., Koelsch, T. L., MacMahon, H., & Lynch, D. A. (2018). **Screening for Lung Cancer: Incidental Pulmonary Parenchymal Findings.** *American Journal of Roentgenology*, *210*(3), 503–513. https://doi.org/10.2214/AJR.17.19003

Domino, K. B. (2019). **Pre-emergence Oxygenation and Postoperative Atelectasis.** *Anesthesiology*, *131*(4), 771–773. https://doi.org/10.1097/ALN.0000000000002875

Erickson, B. J., Korfiatis, P., Akkus, Z., & Kline, T. L. (2017). **Machine Learning for Medical Imaging.** *RadioGraphics*, *37*(2), 505–515. https://doi.org/10.1148/rg.2017160130

Foley, R. W., Nassour, V., Oliver, H. C., Hall, T., Masani, V., Robinson, G., Rodrigues, J. C. L., & Hudson, B. J. (2021). **Chest X-ray in suspected lung cancer is harmful.** *European Radiology*, *31*(8), 6269–6274. https://doi.org/10.1007/s00330-021-07708-0

Fonti, R., Conson, M., & Del Vecchio, S. (2019). **PET/CT in radiation oncology.** *Seminars in Oncology*, *46*(3), 202–209. https://doi.org/10.1053/j.seminoncol.2019.07.001

Ganem, J., Thureau, S., Gardin, I., Modzelewski, R., Hapdey, S., & Vera, P. (2018). **Delineation of lung cancer with FDG PET/CT during radiation therapy.** *Radiation Oncology (London, England)*, *13*(1), 219. https://doi.org/10.1186/s13014-018-1163-2

Gordienko, Y., Gang, P., Hui, J., Zeng, W., Kochura, Y., Alienin, O., Rokovyi, O., & Stirenko, S. (2019). **Deep learning with lung segmentation and bone shadow exclusion techniques for chest X-ray analysis of lung cancer.** In Z. Hu, S. Petoukhov, I. Dychka, & M. He (Eds.), *Advances in Intelligent Systems and Computing* (Vol. 754). Springer International Publishing. https://doi.org/10.1007/978-3-319-91008-6_63

Gorospe, L., Jover-Díaz, R., Muñoz-Molina, G. M., Cabañero-Sánchez, A., Gambí-Pisonero, E., & Barbolla-Díaz, I. (2018). **Round atelectasis: PET/CT findings.** *Internal and Emergency Medicine*, *13*(7), 1127–1128. https://doi.org/10.1007/s11739-018-1867-1

Grott, K., Chauhan, S., & Dunlap, J. D. (2022). **Atelectasis**. In *StatPearls*. StatPearls Publishing, Treasure Island (FL).

Gu, D., Liu, G., & Xue, Z. (2021). **On the performance of lung nodule detection, segmentation and classification.** *Computerized Medical Imaging and Graphics*, *89*(August 2020), 101886. https://doi.org/10.1016/j.compmedimag.2021.101886

Hedenstierna, G., Tokics, L., Reinius, H., Rothen, H. U., Östberg, E., & Öhrvik, J. (2020). **Higher age and obesity limit atelectasis formation during anaesthesia: an analysis of computed tomography data in 243 subjects.** *British Journal of Anaesthesia*, *124*(3), 336–344. https://doi.org/10.1016/j.bja.2019.11.026

Helm, J. M., Swiergosz, A. M., Haeberle, H. S., Karnuta, J. M., Schaffer, J. L., Krebs, V. E., Spitzer, A. I., & Ramkumar, P. N. (2020). **Machine Learning and Artificial Intelligence: Definitions, Applications, and Future Directions.** *Current Reviews in Musculoskeletal Medicine*, *13*(1), 69–76. https://doi.org/10.1007/s12178-020-09600-8

Ibitoye, B. O., Idowu, B. M., Ogunrombi, A. B., & Afolabi, B. I. (2018). **Ultrasonographic quantification of pleural effusion: comparison of four formulae.** *Ultrasonography (Seoul, Korea)*, *37*(3), 254–260. https://doi.org/10.14366/usg.17050

Kumar Basak, S., Wotto, M., & Bélanger, P. (2018). **E-learning, M-learning and D-learning: Conceptual definition and comparative analysis.** *E-Learning and Digital Media*, *15*(4), 191–216. https://doi.org/10.1177/2042753018785180

Kundu, R., Das, R., Geem, Z. W., Han, G.-T., & Sarkar, R. (2021). **Pneumonia detection in chest X-ray images using an ensemble of deep learning models**. *PLOS ONE*, *16*(9), e0256630. https://doi.org/10.1371/journal.pone.0256630

Lin, S., Kantor, R., & Clark, E. (2021). **Coronavirus Disease 2019**. *Clinics in Geriatric Medicine*, *37*(4), 509–522. https://doi.org/10.1016/j.cger.2021.05.001

Lou, Q., Zhang, S.-X., & Yuan, L. (2021). **Clinical analysis of adenovirus pneumonia with pulmonary consolidation and atelectasis in children**. *The Journal of International Medical Research*, *49*(2), 300060521990244. https://doi.org/10.1177/0300060521990244

Maki, R., Miyajima, M., Ogura, K., Tada, M., Takahashi, Y., Arai, W., Adachi, H., & Watanabe, A. (2020). **Pulmonary vessels and bronchial anatomy of the left lower lobe.** *Surgery Today*, *50*(9), 1081–1090. https://doi.org/10.1007/s00595-020-01991-y

Malloy, M. H., & Mcgovern, J. P. (2018). **Hyaline membrane disease (HMD): an historical and Oslerian perspective.** *Journal of Perinatology : Official Journal of the California Perinatal Association*, *38*, 1602–1606. https://doi.org/10.1038/s41372-018-0237-1

Marini, J. J. (2019). **Acute Lobar Atelectasis.** *Chest*, *155*(5), 1049–1058. https://doi.org/10.1016/j.chest.2018.11.014

Martí, A., Morón, S., González, E., & Rojas, J. (2020). **Incidental findings of COVID-19 in F18-FDG PET/CT from asymptomatic patients with cancer in two healthcare institutions in Bogotá, Colombia.** *Biomedica : Revista Del Instituto Nacional de Salud*, *40*(Supl. 2), 27–33. https://doi.org/10.7705/biomedica.5833

Mascalchi, M., Camiciottoli, G., & Diciotti, S. (2017). **Lung densitometry: why, how and when.** *Journal of Thoracic Disease*, *9*(9), 3319–3345. https://doi.org/10.21037/jtd.2017.08.17

McPherson, C., & Wambach, J. A. (2018). **Prevention and Treatment of Respiratory Distress Syndrome in Preterm Neonates.** *Neonatal Network*, *37*(3), 169–177. https://doi.org/10.1891/0730-0832.37.3.169

Mittal, A., Hooda, R., & Sofat, S. (2017). **Lung field segmentation in chest radiographs: a historical review, current status, and expectations from deep learning.** *IET Image Processing*, *11*(11), 937–952. https://doi.org/10.1049/iet-ipr.2016.0526

Norikane, T., Yamamoto, Y., Mitamura, K., Tani, R., & Nishiyama, Y. (2020). **False-Positive 18F-FDG and 18F-Fluorothymidine Uptake in a Patient With Round Atelectasis.** *Clinical Nuclear Medicine*, *45*(3), e158–e159. https://doi.org/10.1097/RLU.0000000000002864

Ozturk, K., Soylu, E., & Topal, U. (2018). **Linear Atelectasis around the Hilum on Chest Radiography: A Novel Sign of Early Lung Cancer**. *Journal of Clinical Imaging Science*, *8*(1), 27. https://doi.org/10.4103/jcis.JCIS_35_18

Petite Felipe, D. J., Rivera Campos, M. I., San Miguel Espinosa, J., Malo Rubio, Y., Flores Quan, J. C., & Cuartero Revilla, M. V. (2021). **Hallazgos iniciales en la radiografía de tórax como predictores de empeoramiento en la infección pulmonar por SARS-CoV-2. Correlación en 265 pacientes.** *Radiología*, *63*(4), 324–333. https://doi.org/10.1016/j.rx.2021.03.004

Pogue, B. W., & Wilson, B. C. (2018). **Optical and x-ray technology synergies enabling diagnostic and therapeutic applications in medicine.** *Journal of Biomedical Optics*, *23*(12), 1–17. https://doi.org/10.1117/1.JBO.23.12.121610

Pritchett, M. A., Lau, K., Skibo, S., Phillips, K. A., & Bhadra, K. (2021). **Anesthesia considerations to reduce motion and atelectasis during advanced guided bronchoscopy.** *BMC Pulmonary Medicine*, *21*(1), 240. https://doi.org/10.1186/s12890-021-01584-6

Protić, A., Bura, M., & Juričić, K. (2020). **A 23-year-old man with left lung atelectasis treated with a targeted segmental recruitment maneuver: a case report.** *Journal of Medical Case Reports*, *14*(1), 77. https://doi.org/10.1186/s13256-020-02409-6

Regmi, P. R., Amatya, I., Kafle, B., Kayastha, P., & Paudel, S. (2021). **Right Sided Aortic Arch with Aberrant Left Subclavian Artery from Kommerell's Diverticulum, a Cause of Persistent Dysphagia in an Adult: A Case Report.** *Journal of Institute of Medicine Nepal*, *43*(1), 47–49. https://doi.org/10.3126/jiom.v43i1.37472

Ruaro, B., Salton, F., Braga, L., Wade, B., Confalonieri, P., Volpe, M. C., Baratella, E., Maiocchi, S., & Confalonieri, M. (2021). **The History and Mystery of Alveolar Epithelial Type II Cells: Focus on Their Physiologic and Pathologic Role in Lung.** *International Journal of Molecular Sciences*, *22*(5), 2566. https://doi.org/10.3390/ijms22052566

Santos. A, S. K. C. V. et al. (2019). **Atelectasis and lung changes in preterm neonates in the neonatal period : a blind radiological report and clinical findings.** *Revista Brasileira de Terapia Intensiva*, *31*(3), 347–353. https://doi.org/10.5935/0103-507X.20190047

Shekhda, K. M. (2020). **A mysterious lesion on the chest X-Ray.** *European Journal of Internal Medicine*, *75*(January), 99–100. https://doi.org/10.1016/j.ejim.2020.02.026

Stengel, D., Leisterer, J., Ferrada, P., Ekkernkamp, A., Mutze, S., & Hoenning, A. (2020). **Point-of-care ultrasonography for diagnosing thoracoabdominal injuries in patients with blunt trauma.** *Emergencias : Revista de La Sociedad Espanola de Medicina de Emergencias*, *32*(4), 280–281. https://doi.org/10.1002/14651858.CD012669.pub2.www.cochranelibrary.com

Sum, S., Peng, Y., Yin, S., Huang, P., Wang, Y., Chen, T., Tung, H., & Yeh, C. (2019). **Using an incentive spirometer reduces pulmonary complications in patients with traumatic rib fractures: a randomized controlled trial.** *Trials*, *20*(1), 797. https://doi.org/10.1186/s13063-019-3943-x

Sun, X. W., Lin, Y. N., Ding, Y. J., Li, S. Q., Li, H. P., & Li, Q. Y. (2021). **Bronchial Variation: Anatomical Abnormality May Predispose Chronic Obstructive Pulmonary Disease.** *International Journal of Chronic Obstructive Pulmonary Disease*, *Volume 16*, 423–431. https://doi.org/10.2147/COPD.S297777

Suzuki, K. (2017). **Overview of deep learning in medical imaging.** *Radiological Physics and Technology*, *10*(3), 257–273. https://doi.org/10.1007/s12194-017-0406-5

Takimoto, T., Kagawa, T., Tachibana, K., Arai, T., & Inoue, Y. (2020). **Massive atelectasis by mucoid impaction in an asthma patient during treatment with anti-interleukin-5 receptor antibody.** *Respirology Case Reports*, *8*(6), e00599. https://doi.org/10.1002/rcr2.599

Tamura, M., Matsumoto, I., Tanaka, Y., Saito, D., Yoshida, S., & Takata, M. (2021). **Predicting recurrence of non-small cell lung cancer based on mean computed tomography value.** *Journal of Cardiothoracic Surgery*, *16*(1), 128. https://doi.org/10.1186/s13019-021-01476-0

Thorpe, A., Rodrigues, J., Kavanagh, J., Batchelor, T., & Lyen, S. (2020). **Postoperative complications of pulmonary resection.** *Clinical Radiology*, *75*(11), 876.e1-876.e15. https://doi.org/10.1016/j.crad.2020.05.006

Ugalde, I. T., Prater, S., Cardenas-Turanzas, M., Sanghani, N., Mendez, D., Peacock, J., Guvernator, G., Koerner, C., & Allukian, M. (2021). **Chest x-ray vs. computed tomography of the chest in pediatric blunt trauma.** *Journal of Pediatric Surgery*, *56*(5), 1039–1046. https://doi.org/10.1016/j.jpedsurg.2020.09.003

Unger, S. A., & Bogaert, D. (2017). T**he respiratory microbiome and respiratory infections.** *Journal of Infection*, *74*, S84–S88. https://doi.org/10.1016/S0163-4453(17)30196-2

Valdés Bécares, J., Martínez García, P., & Maderuelo Riesco, I. (2018). **Atelectasia por tapón de moco resuelta de manera conservadora.** *Atención Primaria*, *50*(9), 562–563. https://doi.org/10.1016/j.aprim.2018.03.006

Warren, M. A., Zhao, Z., Koyama, T., Bastarache, J. A., Shaver, C. M., Semler, M. W., Rice, T. W., Matthay, M. A., Calfee, C. S., & Ware, L. B. (2018). **Severity scoring of lung oedema on the chest radiograph is associated with clinical outcomes in ARDS.** *Thorax*, *73*(9), 840–846. https://doi.org/10.1136/thoraxjnl-2017-211280

Wilson, J. S., Alvarez, J., Davis, B. C., & Duerinckx, A. J. (2018). **Cost-effective teaching of radiology with preclinical anatomy.** *Anatomical Sciences Education*, *11*(2), 196–206. https://doi.org/10.1002/ase.1710

Yin, D., Lu, J., Wang, J., Yan, B., & Zheng, Z. (2021). **Analysis of the therapeutic effect and prognosis in 86 cases of rib fractures and atelectasis.** *Journal of Orthopaedic Surgery and Research*, *16*(1), 86. https://doi.org/10.1186/s13018-021-02221-y